Inorganic Chemistry

Communication

pubs.acs.org/IC

Second-Coordination-Sphere Effects Increase the Catalytic Efficiency of an Extended Model for $Fe^{III}M^{II}$ Purple Acid Phosphatases

Bernardo de Souza,*[,†] Gabriel L. Kreft,[‡] Tiago Bortolotto,[‡] Hernán Terenzi,[‡] Adailton J. Bortoluzzi,[†] Eduardo E. Castellano,[§] Rosely A. Peralta,[†] Josiel B. Domingos,[†] and Ademir Neves*[,†]

[†]Departamento de Química and [‡]Departamento de Bioquímica, Universidade Federal de Santa Catarina, Florianópolis, Santa Catarina 88040-900, Brazil

[§]Departamento de Física e Informática, Universidade de São Paulo, São Carlos 13566-590, Brazil

Supporting Information

ABSTRACT: Herein we describe the synthesis of a new heterodinuclear $Fe^{III}Cu^{II}$ model complex for the active site of purple acid phosphatases and its binding to a polyamine chain, a model for the amino acid residues around the active site. The properties of these systems and their catalytic activity in the hydrolysis of bis(2,4-dinitrophenyl)phosphate are compared, and conclusions regarding the effects of the second coordination sphere are drawn. The positive effect of the polymeric chain on DNA hydrolysis is also described and discussed.

Over many years, great efforts have been made to synthesize small molecules that can model the catalytic activity of many important enzymes. Phosphatases, esterases, oxidases, and a variety of other enzymes have been successfully modeled through organic molecules or metal complexes that can reproduce their physicochemical properties and even their catalytic activity, albeit with a much lower efficiency.[1]

As has been suggested, this discrepancy between the catalytic efficiencies of model compounds and true enzymes is, to a large extent, due to the lack of many important intermolecular interactions of the second coordination sphere of the model systems in comparison to the enzyme.[2] In many cases, the amino acid residues close to the active site are known to be necessary for efficient enzymatic activity because mutation of these residues can cause deactivation or even inactivation of the catalyst.[3]

One such case is purple acid phosphatases (PAPs), where histidine residues around the $Fe^{III}M^{II}$ active site have been shown to play an important role in substrate binding and activation. Mutations of His195 to Ala in the second sphere in kidney bean PAP resulted in a sharp decrease in activity,[3] and recent theoretical studies have reinforced the importance of these proximal histidine residues to properly describe coordination of the substrate and stabilization of the transition state (TS).[4a] Moreover, a recent $Fe^{III}Fe^{II}$ model complex composed of secondary ammonium groups presented the highest catalytic efficiency (k_{cat}/K_M) ever reported for a PAP model in relation to phosphate diester hydrolysis, thus reinforcing the second-sphere argument.[4b]

In this context, over the past decade our group has reported a series of $Fe^{III}M^{II}$ complexes (M^{II} = Fe, Zn, Cu, Ni, Mn, Co, Hg, Cd) containing the unsymmetrical ligand H_2L = 2-bis{[(2-pyridylmethyl)aminomethyl]-6-[(2-hydroxybenzyl)(2-pyridylmethyl)]aminomethyl}-4-methylphenol as functional and structural models for the active site of PAPs,[1,5] with structural and electronic properties very similar to those reported for the corresponding enzymes. The most important feature in these systems is that the dinuclear mixed-valence ($Fe^{III}M^{II}$) catalyst contains a labile $M^{II}OH_2$ site for substrate binding and an adjacent $Fe^{III}OH$ group as the initiating nucleophile, which can be generated at pH values close to 7.0. Additionally, the mechanism of phosphate diester bond cleavage in the DNA model substrate BDNPP and in DNA itself by these complexes has been reasonably well established.[1,5] Nevertheless, as observed in other model complexes, their overall catalytic efficiency in phosphate diester hydrolysis is still much lower than that of the target enzymes.

In this paper, we propose extending the PAP models by adding the $Fe^{III}Cu^{II}L^1$ unit (with FeCu being the most active within the $Fe^{III}M^{II}$ series) to a small polyethyleneimine chain (PEI; 1200 Da) with the aim of emulating the microenvironment around the active site (Figure S4 in the Supporting Information, SI). The ligand H_2L was modified to H_2L^1, with a carbonyl attached to the terminal phenol (see the SI), and its $Fe^{III}Cu^{II}L^1$ complex was obtained (Figure 1). In a previous study, the $Fe^{III}Zn^{II}L^1$ complex was bound to heterogeneous (3-aminopropyl)silica, and a smaller K_M in the hydrolysis of BDNPP was obtained as a result of secondary interaction effects.[6] Here we use PEI anchored to the $Fe^{III}Cu^{II}L^1$ complex in order to mimic histidine residues in the polypeptide chain, to

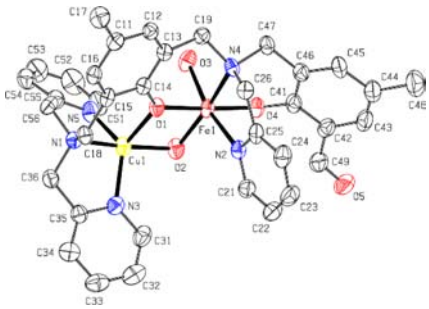

Figure 1. ORTEP plot of the cation complex of **1**.

Received: January 4, 2013
Published: March 15, 2013

   dx.doi.org/10.1021/ic400025j | *Inorg. Chem.* 2013, 52, 3594−3596

increase the water solubility of the catalyst, and to increase the interactions with the DNA framework because at neutral pH PEI is positively charged.

The FeCuL[1] (**1**) X-ray structure presented close similarity to that of FeZnL[1], with a dinuclear $Fe^{III}(\mu\text{-OH})Cu^{II}L^1$ unit where the Fe−Cu distance is 3.053(11) Å (see Table S1 in the SI). The complex also presented a coordinated water molecule at the iron center [Fe−O3 = 2.070(5) Å], which is proposed to act as the nucleophile in FeZnL[1] and $Fe^{III}M^{II}L$ complexes. It is important to note that the aldehyde group is not coordinated to any metal, and so it is free to react with PEI. In the UV/vis spectrum of **1** in CH_3CN (Figure S5 in the SI), there is a ligand-to-metal charge transfer (LMCT) centered at 546 nm (ε = 2100 L mol^{-1} cm^{-1}) typical of these systems and very similar to that of the FeCu-substituted PAP, which has a λ_{max} at 545 nm (ε = 3400 L mol^{-1} cm^{-1}).[7]

To obtain the **1**/PEI (**1-PEI**) system, a stock solution of **1** in dimethyl sulfoxide was added to a PEI solution in water at a 1:1 polymer chain per complex molecule ratio. The appearance of the conjugated imine band was monitored until completeness (Figures S6 and S7 in the SI). During formation of the imine, no changes were observed in the phenolate-to-Fe^{III} LMCT, indicating that the coordination sphere of the metals remains unchanged when **1** is anchored to PEI. A similar experiment was carried out using the corresponding GaZnL[1] complex (see the SI) as a ^1H NMR probe, and the disappearance of the aldehyde peak at 9.75 ppm was monitored. After imine formation, no changes were observed even after 1 week (Figures S8 and S9 in the SI).

Potentiometric titration of **1** in CH_3CN/H_2O (1:1, v/v) resulted in three deprotonation constants: pK_{a1} = 3.12, pK_{a2} = 5.26, and pK_{a3} = 8.45, similar to those obtained for FeZnL,[1a] where the first refers to the hydroxo bridge formation and the second and third to the terminal water molecules coordinated respectively to the Fe^{III} and Cu^{II} centers (Figure S10 in the SI). Spectrophotometric titrations under the same conditions resulted in pK_a's similar to those for **1** (Table S2 in the SI), and the two kinetically relevant protonations of the **1-PEI** system were obtained, pK_{a2} = 5.09 and pK_{a3} = 7.35 (Figure S11 in the SI), indicating that the influence of the polyamine chain in terms of pK_a is mainly related to a lowering of the value of the copper-coordinated water.

In fact, the pK_a values obtained correspond well to the observed profile of activity in BDNPP hydrolysis versus the pH (Figure S12 in the SI), with **1-PEI** having a maximum at pH ~6, one unit lower than that of **1**. This more acidic optimum pH was to be expected because the positive charges of the polyamine stabilize the terminal hydroxides formed and increase the $K_{ass.}$ value of the substrate at lower pH values. The good correlation observed between the titrated pK_a values and the activity profile suggests that the active species are the same in both cases, that is, $[Fe(OH)(\mu\text{-OH})Cu(H_2O)L^1]^+$, as proposed for other $Fe^{III}M^{II}$ complexes containing the ligand H_2L.[1,5] This maximum value for **1-PEI** also correlates better than that of **1** with the activity of PAPs at acid pH, indicating regulation of the second-sphere effects at the optimum pH through the pK_a of the metal-coordinated water.

A Michaelis−Menten plot at each maximum pH provided further insight into the influence of second-sphere amines (Figure 2). For the FeCu complex **1**, $k_{cat.}$ = 6.77 ± 0.04 h^{-1} and K_M = 3.08 ± 0.03 mM at 323 K, values that are similar to those for FeZnL[1] and typical of the $Fe^{III}M^{II}$ series with H_2L. For the **1-PEI** system, $k_{cat.}$ = 1.14 ± 0.09 h^{-1} and K_M = 0.40 ± 0.13 mM. These parameters show that, although **1-PEI** is less active than **1**, it has a much stronger coordination with the substrate. The overall result is that the **1-PEI** system has a higher efficiency ($k_{cat.}/K_M$) than **1** and the highest association constant of the PAP models reported to date. Indeed, the increase in the association constant is coherent with previous studies on the role of second-sphere histidines.[2−4] In terms of substrate conversion, complex **1** presented 7 turnovers, at 25 μM and 323 K, after 24 h in a 2 mM solution of BDNPP, while **1-PEI** presented 22 turnovers, probably because of the increase in the $K_{ass.}$ value when complex **1** was bound to PEI. The deuterium kinetic isotopic effect k_H/k_D was found to be 1.52 for **1** and 1.21 for **1-PEI** (Figures S13 and S14 in the SI).

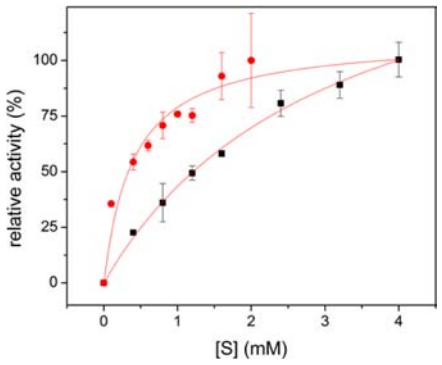

Figure 2. Michaelis−Menten plot of **1** (pH 7) and **1-PEI** (pH 6) in water: (■) **1**; (●) **1-PEI**. T = 323 K; [I] = 1 M; [**1**] = 25 μM, and [**1-PEI**] = 5 μM.

Substrate binding at the Cu^{II} center could be assigned because of the small change observed in the phenolate-to-Fe^{III} LMCT when the phosphate diester was added to **1** or **1-PEI** (Figure S15 in the SI). On the basis of these results and on previous studies of the $Fe^{III}M^{II}$ series, we propose that the same mechanism associated with FeZnL[1], where the substrate binds to M^{II} and the Fe^{III} terminal hydroxide acts as the nucleophile (as in Figure S4 in the SI), may be operating in the catalytic systems presented herein.

To evaluate the influence of the model chain on stabilization of the TS, Eyring plots of **1** and **1-PEI** were obtained (Figure S16 in the SI) after kinetic experiments were carried out at 35, 40, 45, and 50 °C. From the differences between the parameters when the reaction is catalyzed by **1** and H_2O (Table 1), one can clearly see that the effect of the complex on the process is basically entropic. It favors the reaction by approximating the substrate to the nucleophile, resulting in a $\Delta S^{‡}$ value close to that observed for unimolecular reactions.

Table 1. Activation Parameters Obtained from Eyring Plots

	$\Delta H^{‡}$ (kJ mol^{-1})	$-T\Delta S^{‡}$ (kJ mol^{-1})[a]	$\Delta G^{‡}$ (kJ mol^{-1})[a]
H_2O[b]	79.4	−34.4	113.8
1[c]	83.6 ± 0.4	−12.6 ± 0.4	96.2 ± 0.5
1-PEI[d]	39.1 ± 0.1	−61.9 ± 0.1	101 ± 0.1

[a]At 323 K. [b]Reference 9. [c]At pH 7. [d]At pH 6.

The influence of the polymer chain can thus be assumed to derive from two different effects. It significantly lowers the $\Delta H^{‡}$ energy barrier by possibly forming hydrogen bonds and stabilizing the negatively charged TS, but it also makes $\Delta S^{‡}$ much more unfavorable because of the need for reorganization around the TS in every cycle, thus increasing $\Delta G^{‡}$ and lowering

dx.doi.org/10.1021/ic400025j | Inorg. Chem. 2013, 52, 3594−3596

$k_{cat.}$ as observed. It should be noted that if the second sphere of **1-PEI** were more "rigid" (as in an enzyme) and the $\Delta S^{\ddagger}$ value of the system were close to that observed for **1**, one would expect a $k_{cat.}$ value of above 8000 s^{-1}, which lies within the enzymatic range. Indeed, these results highlight the enormous influence of the second-sphere effects on enzyme models and demonstrate that, in principle, it is possible to achieve much higher catalytic activities when suitable interactions between the first and second coordination spheres are available.[3,4]

Following the results obtained by FeZnL[5d] and considering that PEI has a high affinity toward the polyanion DNA,[9] the catalytic activity of the complex was assayed (Figure S19 in the SI). In these studies, the activity of FeCuL (**2**; see the SI) without the aldehyde and incapable of covalent binding to PEI was used as an internal control. The results show a clear influence of the linked polymer on the cleavage of **1** with the control (unmodified PEI) having negligible activity (Table 2).

Table 2. Percentage of FII after 24 h at pH 7 and 310 K

[C] (μM)	**2**	**2+PEI**	factor	**1**	**1-PEI**	factor
1	2.5	5.8	2.3×	2.2	17.1	6.8×
2.5	7.9	10.5	1.3×	3.8	27.6	7.3×
10	18.6	21.6	1.2×	10.2	45.0	4.4×

A pseudo-Michaelis–Menten plot was obtained using the observed first-order rate constant (k_{obs}) versus [C]. Values of $k_{cat.}$ = 0.12 h^{-1} and K_M = 19.5 μM were obtained for **1** and $k_{cat.}$ = 0.13 h^{-1} and K_M = 4.8 μM were obtained for **1-PEI** (Figures S20 and S21 in the SI). The stronger association observed for **1-PEI** is consistent with the results obtained with BDNPP, and the value of $k_2/K_M = 2.7 \times 10^4$ h^{-1} M^{-1} is thus the highest ever reported for PAP models capable of cleaving plasmid DNA.

To assess the pathway of the reaction, inhibitors of radical species were used in the reaction medium, and the results indicated minor oxidative cleavage events with a major hydrolytic pathway (Figures S22–S24 in the SI). No DNA groove binding preferences for either **1** or **1-PEI** (Figures S25 and S26 in the SI) were detected. Further studies are being conducted to better understand the DNA cleavage ability of **1** and **1-PEI**. Chemical modifications to the polymer are being made to simulate other important amino acids in the second sphere.

In conclusion, the addition of a polymer to mimic the second coordination sphere around the active site has proven to be a simple and elegant solution to increasing the activity of model complexes. It also revealed a possible way to enhance DNA cleavage through a higher association constant, improving the overall efficiency. Further studies involving the synthesis of complexes **GaZn-PEI** and **GaCu-PEI**, their interaction with DNA, and their cytotoxic activity in adenocarcinoma cells are underway and will be the subject of a full paper.

■ ASSOCIATED CONTENT

Supporting Information

X-ray crystallographic data in CIF format for **1**, synthesis and characterization of **1**, Tables S1–S3, and Figures S1–S27. This material is available free of charge via the Internet at http://pubs.acs.org.The atomic coordinates for **1** have also been deposited with the Cambridge Crystallographic Data Centre as CCDC 917883. The coordinates can be obtained, upon request, from the Director, Cambridge Crystallographic Data Centre, 12 Union Road, Cambridge CB2 1EZ, U.K.

■ AUTHOR INFORMATION

Corresponding Author

*E-mail: ademir.neves@ufsc.br. Phone: +55 (48) 3721-6844 R219.

Notes

The authors declare no competing financial interest.

■ ACKNOWLEDGMENTS

We are grateful to INCT-Catálise, INCT-Biologia Molecular Estrutural e Bioimagem, and CNPq.

■ REFERENCES

(1) (a) Neves, A.; Lanznaster, M.; Bortoluzzi, A. J.; Peralta, R. A.; Casellato, A.; Castellano, E.; Schenk, G. *J. Am. Chem. Soc.* **2007**, *129*, 7486–7487. (b) Mitić, N.; Smith, S. J.; Neves, A.; Guddat, L. W.; Gahan, L. R.; Schenk, G. *Chem. Rev.* **2006**, *106*, 3338–3363.

(2) (a) Mancin, F.; Scrimin, P.; Tecilla, P. *Chem. Commun.* **2012**, *48*, 5545–5559. (b) Williams, N. H.; Takasaki, B.; Wall, M.; Chin, J. *Acc. Chem. Res.* **1999**, *32*, 485–493.

(3) Funhoff, E. G.; Wang, Y.; Andersson, G.; Averill, B. A. *FEBS J.* **2005**, *272*, 2968–2977.

(4) (a) Retegan, M.; Milet, A.; Jamet, H. *J. Phys. Chem. A* **2010**, *114*, 7110–7118. (b) Comba, P.; Gahan, L. R.; Hanson, G. R.; Mereacre, V.; Noble, C. J.; Powell, A. K.; Prisecaru, I.; Schenk, G.; Zajaczkowski-Fisher, M. *Chem.—Eur. J.* **2012**, *18*, 1700–1710.

(5) (a) Xavier, F. R.; Peralta, R. A.; Bortoluzzi, A. J.; Drago, V.; Castellano, E. E.; Haase, W.; Tomkowicz, Z.; Neves, A. *J. Inorg. Biochem.* **2011**, *105*, 1740–1752. (b) Xavier, F. R.; Neves, A.; Casellato, A.; Peralta, R. A.; Bortoluzzi, A. J.; Szpoganicz, B.; Severino, P. C.; Terenzi, H.; Tomkovicz, Z.; Ostrovski, S.; Haase, W.; Ozarowski, A.; Krzystek, J.; Telser, J.; Schenk, G.; Gahan, L. R. *Inorg. Chem.* **2009**, *48*, 7905–7921. (c) Schenk, G.; Peralta, R. A.; Batista, S. C.; Bortoluzzi, A. J.; Szpoganicz, B.; Dick, A. K.; Herrald, P.; Hanson, G. R.; Szilagyi, R. K.; Riley, M. J.; Gahan, L. R.; Neves, A. *J. Biol. Inorg. Chem.* **2008**, *13*, 139–155. (d) Peralta, R. A.; Bortoluzzi, A. J.; de Souza, B.; Jovito, R.; Xavier, F. R.; Couto, R. A. A.; Casellato, A.; Nome, F.; Dick, A.; Gahan, L. R.; Schenk, G.; Hanson, G. R.; de Paula, F. C. S.; Pereira-Maia, E. C.; de P. Machado, S.; Severino, P. C.; Pich, C.; Bortolotto, T.; Terenzi, H.; Castellano, E. E.; Neves, A.; Riley, M. J. *Inorg. Chem.* **2010**, *49*, 11421–11438.

(6) Piovezan, C.; Jovito, R.; Bortoluzzi, A. J.; Terenzi, H.; Fischer, F. L.; Severino, P. C.; Pich, C.; Azzolini, G. G.; Peralta, R. A.; Rossi, L. M.; Neves, A. *Inorg. Chem.* **2010**, *49*, 2580–2582.

(7) Twitchett, M. B.; Schenk, G.; Aquino, M. A. S.; Yiu, D. T.-Y.; Lau, T.; Sykes, A. G. *Inorg. Chem.* **2002**, *41*, 5787–5794.

(8) Bunton, C. A.; Farber, S. J. *J. Org. Chem.* **1969**, *34* (4), 767–772.

(9) Thomas, M.; Klibanov, A. M. *Appl. Microbiol. Biotechnol.* **2003**, *62*, 27–34.